ELSEVIER

Polymer 42 (2001) 9–15

polymer

www.elsevier.nl/locate/polymer

Studies of sulfonated block copolymer and its blends

A. Mokrini, J.L. Acosta*

Instituto de Ciencia y Tecnologia de Polimeros, C/Juan de la cierva 3, 28006 Madrid, Spain

Received 5 March 2000; received in revised form 26 April 2000; accepted 6 May 2000

Abstract

This paper reports the synthesis and characterization of a sulfonated polymer based on hydrogenated poly(styrene–butadiene) block copolymer (HPBS). Block copolymer ionomers were prepared through sulfonation of part of the polystyrene blocks. The free acid samples (HPBS–SH), and their blends with the non-sulfonated polymer (HPBS) and polypropylene (PP) were studied. FTIR was used to confirm sulfonation. DMA and DSC analyses have shown that T_g (HPB) remains constant for all the samples studied. Glass transition temperatures of polystyrene (PS) measured through DMA present an increase of about 30°C after sulfonation, diminution (up to 13°C) when the amount of HPBS increases in HPBS–SH/HPBS blends and augmentation (up to 28°C) as the PP content in HPBS–SH/PP blends increases. Complex impedance measurements have shown that proton conductivity of HPBS–SH was about $8 \times 10^{-3}\ \Omega^{-1}\ cm^{-1}$, lower values were observed generally in the case of blends. Non-isothermal crystallization of PP was studied using Avrami analysis.

Keywords: Hydrogenated poly(butadiene–styrene); Sulfonation; Blends

1. Introduction

Electroactive polymers are recently studied by several investigation groups [1–4]. The interest arises from the possibility of their application in various electrochemical devices working at moderate temperatures.

The poly(butadiene–styrene) block copolymer (PBS) possesses a two-phase microstructure consisting of polystyrene domains dispersed in a rubbery continuous phase [5]. One way to increase the reactivity of the conventional block copolymer thermoplastic elastomers is to crosslink the PS microdomains; but to overcome the cross-linking/cyclization and consequently the instability problems due to the high reactivity of carbon double bonds, hydrogenation was used to limit the amount of unsaturations in the starting polymer to the extent of the desired sulfonation. The sulfonated polymers (HPBS–SH) systems present a new physical network formed by an ion-rich domain.

Several investigations have been devoted to study the morphology, chemical and physical properties of sulfonated HPBS salts [5–8]. In this paper, we focus on the behavior of free acid form of the polymer and its blend with the non-sulfonated starting polymer and polypropylene. Polymer blends have become important to many industries, particularly where a combination of amorphous and semi-crystalline components could produce a property synergism. Polypropylene was selected to increase the dimensional stability and ease of processing of the modified polymer.

2. Experimental

2.1. Materials

The polymer used in this work was a selectively hydrogenated poly(butadiene–styrene) block copolymer leading to an ethylene–butylene–styrene terpolymer (HPBS). The polymer commercially designated Calprene CH-6120, was provided by Repsol and contains 30 wt.% styrene units. Sulfonating reagent was acetyl sulfate prepared by the reaction of acetic anhydride and concentrated sulfuric acid (96%). Sulfonation was carried out in 1,2-dichloroethane, previously dried using molecular sieves to remove any water that might have been present.

2.2. Sulfonation procedure

Acetyl sulfate preparation: First, acetic anhydride was cooled below −10°C, and the corresponding volume of 96% sulfuric acid was added. The solution was stirred, and finally 1,2-dichloroethane (DCE) was added. The

* Corresponding author. Tel.: +34-91-562-2900; fax: +34-91-564-4853.
E-mail address: icta320@ictp.csic.es (J.L. Acosta).

0032-3861/01/$ - see front matter
PII: S0032-3861(00)00353-0

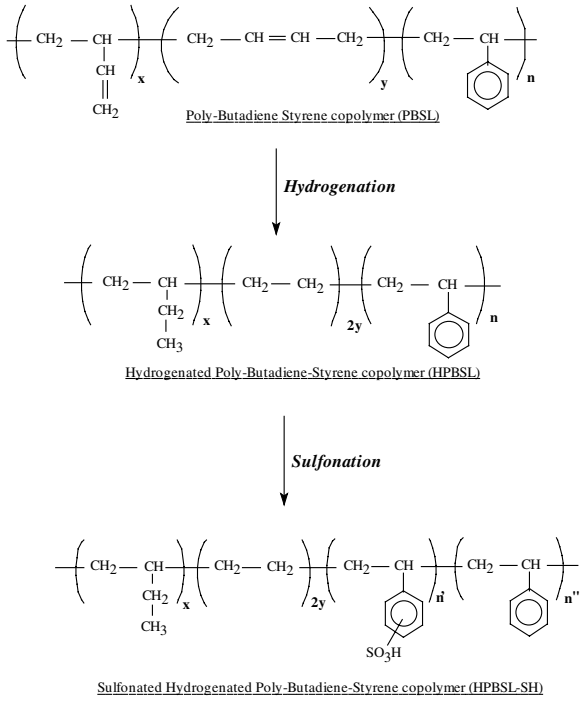

Fig. 1. Chemical mechanisms of sulfonation reaction of hydrogenated poly(butadiene–styrene) block copolymer.

product obtained was maintained at 0°C in an ice bath, until its addition to the reaction medium.

Sulfonation reaction: Sulfonation was carried out according to the procedure described by Makowski et al. [10,11]. In an agitated reactor, the polymer was dissolved in DCE at 52–56°C and purged with nitrogen. Then, acetyl sulfate prepared as described above was added. The solution was stirred and purged with nitrogen during the experiment. Samples were removed at the desired reaction times and precipitated in methanol or deionized water (1 l per 10 g of the polymer used). The highly sulfonated polymer was partially soluble in methanol or water, which was recovered by steam stripping, and vacuum dried at 50–60°C for few days.

The complete removal of residual acid from the final product after sulfonation is important since it can interfere with the properties of the final product. The dried polymer was cut into small pieces, washed once with boiling deionized water, and many times with cold water till neutral pH of the sewage was obtained. It was finally vacuum dried at 50–60°C for the last time.

The titration of the polymer against a standard potassium hydroxide solution (0.1 N) using phenolphthalein as an indicator, shows a sulfonation level higher than 15%.

2.3. Blending procedure

Two blending procedures were used in this study. For HPBS–SH/HPBS blends, an open two-roll mill (fraction 1:1.4) was utilized, using a conventional mixing procedure.

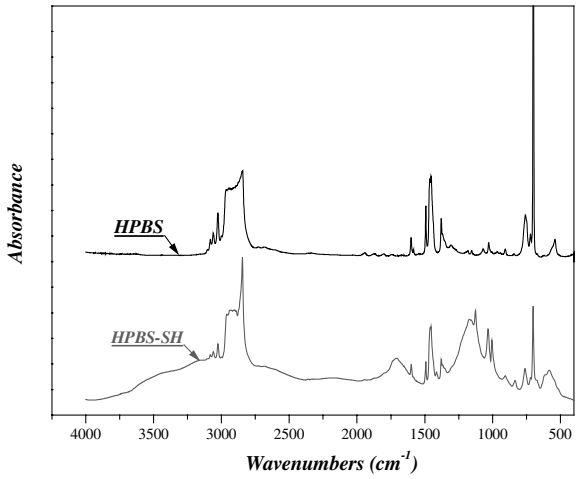

Fig. 2. FTIR spectra of HPBS before and after sulfonation. Resolution settings: 4 cm^{-1}, 32 scans.

The blending time was 20 min to maximize intermixing of the polymers.

For the preparation of HPBS–SH/polypropylene (HPBS–SH/PP) blend, a Brabender torque rheometer was used. First, PP was melted in the thermoplastic mixing chamber preheated at 180°C, then HPBS–SH was added using a rotor speed of 60 rpm. The material remained in the mixing chamber for 10 min to ensure homogenization. The blends were molded into a film with a thickness of 200–400 μm in a Collin 600 hydraulic press.

2.4. Analysis

A Nicolet 520 Fourier-transform IR (FTIR) spectrometer was used to record the infrared spectra of HPBS polymer before and after sulfonation. A resolution setting of 4 cm^{-1} and 32 scans were utilized. Samples were cast as thin films.

A Mettler Differential Scanning Calorimeter 30 (DSC) apparatus calibrated with indium was used for the thermal analysis of the samples. To determine the glass transition (T_g), samples were first heated to 250°C at 30°C/min, then cooled to −140°C at 100°C/min, held at this temperature for 5 min, and then scanned at 10°C/min from −140 to 250°C. For the non-isothermal crystallization, samples were heated to 250°C at 30°C/min, held at this temperature for 2 min, and then scanned at slow rates from 250 to 40°C. The scanning rates used were 2, 4, 6, 8 and 10°C/min. All the measurements were made under a nitrogen atmosphere.

Dynamic mechanical analysis (DMA) measurements were performed with a TA Instrument 2980 Dynamic Mechanical Analyzer, operating at the fixed frequency and film tension mode. The frequency used was 0.1 Hz and the temperature was varied from −100 to 300°C at a heating rate of 5°C/min. The samples for DMA analysis were prepared by compression molding at 150°C.

A Hewlett Packard 4192A Impedance Spectroscopy Analyzer controlled by a computer was used for impedance

Table 1
List of the materials

Designation	HPBS–SH (wt%)	HPBS (wt%)	PP (wt%)
AM-10	100	–	–
AM-11	90	10	–
AM-12	80	20	–
AM-13	70	30	–
AM-21	90	–	10
AM-22	80	–	20
AM-23	70	–	30
AM-23*	–	70	30

spectroscopic analysis of the samples. Complex impedance measurements were carried out in AC mode, in the frequency range 0.01–10 000 kHz, and 1 V amplitude of the applied AC signal. The samples were painted with Ag thin film (Ceramic luster 200 in xylene supplied by EMETRON), to optimize the electrode–electrolyte interface, and sandwiched between two brass blocking electrodes in the cell measurement.

For impedance analysis, two hydration procedures were used. The first method consists of immersing samples in deionized water at 50°C for 1 h. Before starting the measurements, they were dried up superficially with filter paper, and then placed in the measurement cell. In the second procedure, the measurement cell containing the sample was placed in a closed vessel with steam–water saturated atmosphere.

3. Results and discussion

3.1. HPBS sulfonation and blending

Fig. 1 shows the chemical mechanisms of HPBS sulfonation. FTIR was used to confirm the sulfonation of the styrene groups of the HPBS polymer. Fig. 2 compares a series of FTIR spectra before and after sulfonation. As shown, the changes in the combination vibrations (finger bands) between 1950 and 1650 cm^{-1} particularly characterizes of the phenyl group. The band centered around 1200 cm^{-1} is characteristic of the OySyO asymmetric stretching vibration. The absorbancies at 1005 and 1126 cm^{-1} result, respectively, from the vibrations of phenyl ring substituted with a sulfonate group and sulfonate anion attached to phenyl ring [6].

The sulfonated polymer (HPBS–SH) was kept in its acid form. For this study, blends of HPBS–SH with HPBS and PP have been prepared. Table 1 lists the composition of all the materials used.

3.2. DMA and DSC analysis: glass transition temperatures

DMA methods have been extremely useful for the analysis of the phase behavior of the polymers studied. In Fig. 3, tan δ is plotted as a function of temperature for HPBS–SH/HPBS blends. It can be observed that all the materials analyzed show the presence of two transitions, the lower one is associated with glass transition temperature of the

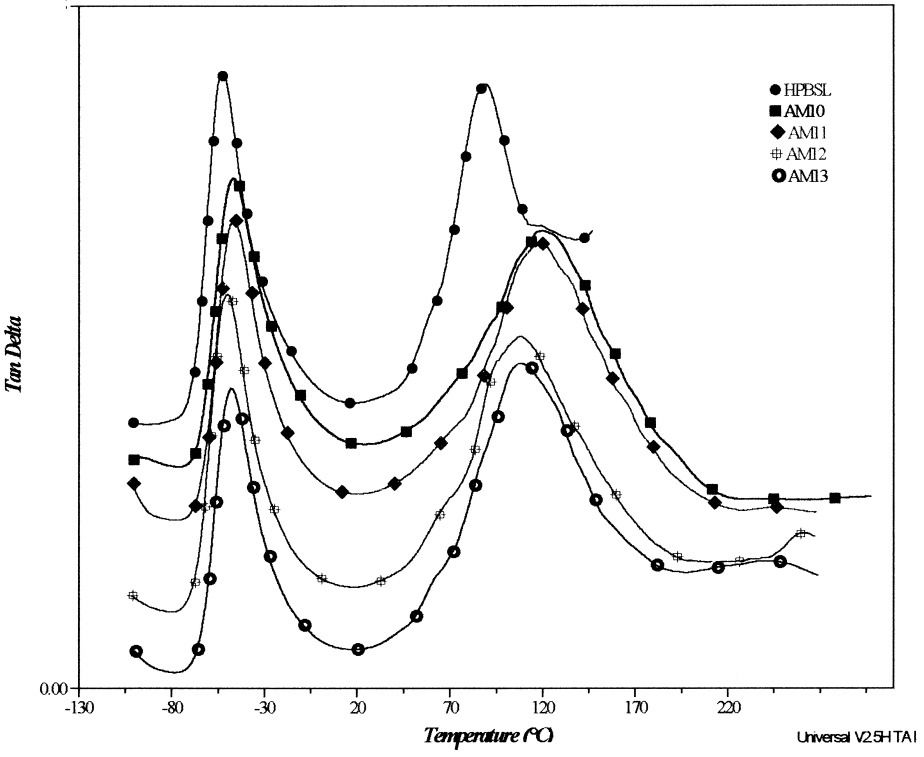

Fig. 3. DMA spectra for HPBS–SH/PBSH blends. Frequency 1 Hz. Temperature range −100 to 290°C. Heating rate 5°C/min.

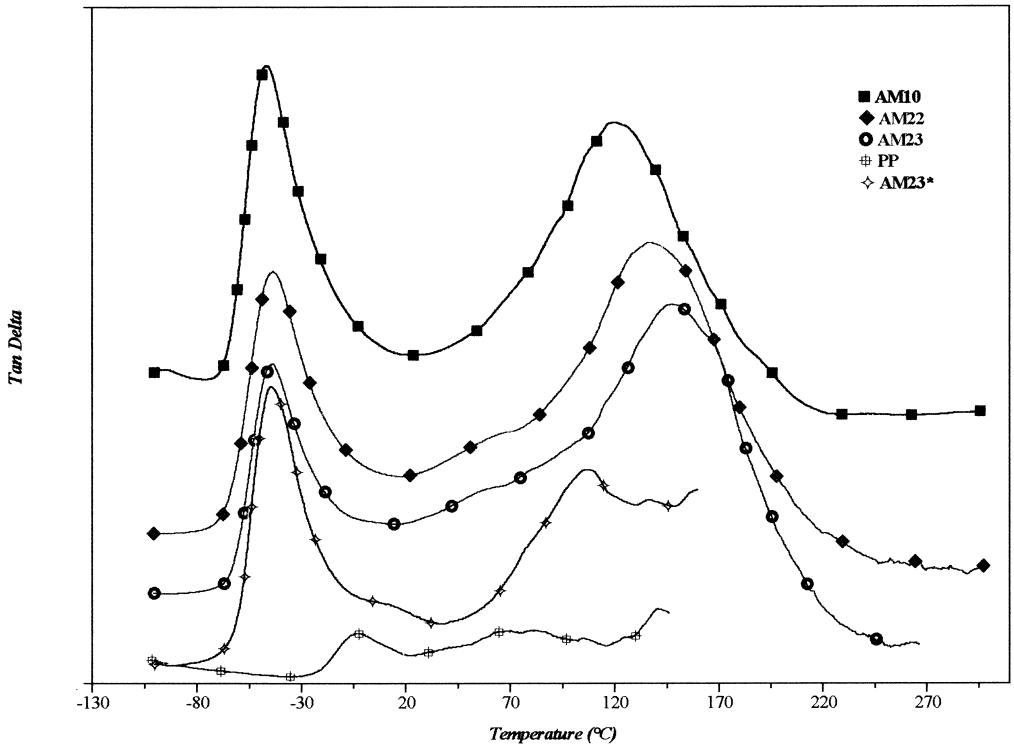

Fig. 4. DMA spectra for HPBS–SH/PP blends. Frequency 1 Hz, Temperature range −100 to 290°C. Heating rate 5°C/min.

hydrogenated polybutadiene HPB, and the higher one with that of polystyrene (PS). In addition, a new transition related to the multiplets or cluster phase is observed in blends containing sulfonated polymer.

Glass transition temperatures, defined as the inflection point in DSC thermograms and as the maximum signal of tan δ in DMA Figs. 3 and 4, are summarized in Table 2.

It can be observed that glass transition temperature associated with hydrogenated polybutadiene units $T_{g(HPB)}$, is insensitive to sulfonation; the maximum variation observed is about 6°C, while $T_{g(PS)}$ related to styrene blocks is increased considerably (+30°C) after sulfonation ($T_{g(PS)} = 90$°C for HPBS and 120°C for HPBS–SH). This increase in glass transition temperature is directly associated to ion content [9]. This is probably a result of the restrictions on the segmental movement in the styrene blocks, due to the introduction of sulfonate groups with the subsequent cross-linking. $T_{g(PS)}$ in HPBS/HPBS–SH blends are included in the range between glass transition temperatures of initial polymers, and decreases while the amount of HPBS added to the sulfonated polymer increases.

Table 2
Glass transition temperatures through DMA and DSC

Sample name	DMA		DSC	
	$T_{g(PS)}$ (K)	$T_{g(PHB)}$ (K)	$T_{g(PHB)}$ (K)	$T_{m(PP)}$ (K)
HPBSL	363.32	222.11	223.45	–
AM-10	393.33	227.10	224.35	–
AM-11	392.12	228.05	224.55	–
AM-12	382.17	224.63	224.25	–
AM-13	380.74	225.04	223.25	–
AM-21	416.28	229.82	224.15	435.55
AM-22	410.62	230.54	222.55	437.05
AM-23	421.80	216.17	223.95	437.95

The transition that occurs between 200 and 300°C is related to ion aggregations or cluster phase, and it was not observed in all the samples (Fig. 3). The disappearance of the transition related to clusters in the high-temperature region indicates that damage was done to this phase of the blend, or changes in structure due to the processing conditions and environmental exposure.

DMA spectra for HPBS–SH/PP blends are represented in Fig. 4. The first observation is the affinity between the two polymer phases, which indicates a partial compatibility of the blends at selected concentrations. In addition, changes in glass transition temperatures are observed; $T_{g(PP)}$ increases from −2.7 to 12.6°C after blending with HPBS.

The same tendency is observed for $T_{g(HPB)}$, while in the case of $T_{g(PS)}$, in addition to the variation due to sulfonation, augmentation up to 28°C is observed due to the incorporation of polypropylene to the sulfonated polymer. An increase in T_g is observed as the PP content increases, as a result of the introduction of crystalline component that limits the chain movements.

The variation of glass transition temperature with the amount of HPBS or PP added to sulfonated polymer HPBS–SH in the blends studied is represented in Fig. 5.

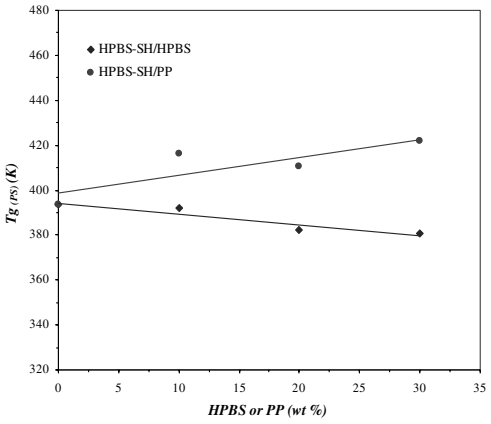

Fig. 5. Variation of PS glass transition temperature measured through DMA, with the amount of HPBS or PP added in HPBS–SH/HPBS and HPBS–SH/PP blends.

3.3. Kinetics of non-isothermal crystallization

The study of the crystallization and melting behavior of crystallizable blends may be a useful way to obtain fundamental information about miscibility, compatibility and microstructural behavior of the polymers mixed. In general, studies of crystallization are limited to ideal conditions, in which external conditions are constant (isothermal crystallization), for an easier theoretical analysis. However, practical processes, such as extrusion, molding and film forming usually occur under dynamic non-isothermal conditions. Hence, it will be useful to have a quantitative evaluation of the non-isothermal crystallization parameters.

The thermograms show that crystallization of pure PP or from the melt HPBS–SH/PP blends, depends greatly upon cooling rates and blend compositions. For a given composition, the crystallization process begins at higher temperatures when slower scanning rates are used. At a given cooling rate, the presence of HPBS–SH reduces the overall PP crystallization rate.

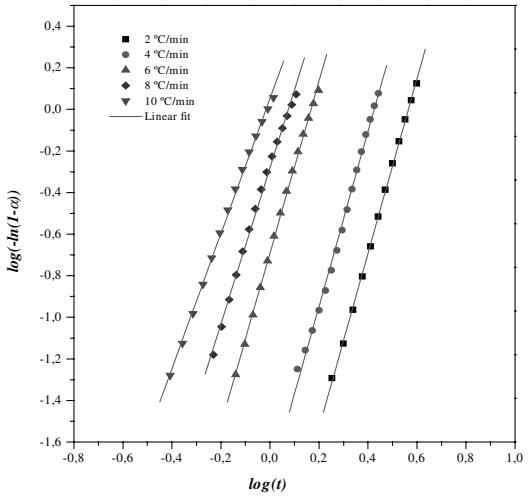

Fig. 6. Representation of the Avrami equation, for AM-21 blend at different scanning rates.

Table 3
Kinetic parameters obtained from the application of the Avrami equation for non-isothermal crystallization

Sample	β (°C/min)	log K	n	R
AM-21	2	−2.37	4.3	99.97
	4	−1.79	4.2	99.78
	6	−0.69	4.1	99.94
	8	−0.28	3.8	99.79
	10	0.05	3.3	99.90
AM-22	2	−2.84	4.5	99.92
	4	−1.59	4.4	99.91
	6	−0.74	4.3	99.84
	8	−0.32	4.1	99.53
	10	−0.01	3.7	99.47
AM-23	2	−3.24	4.9	99.91
	4	−1.92	4.8	99.81
	6	−1.08	4.5	99.52
	8	−0.63	4.2	99.27
	8	−0.36	3.9	99.06
PP	2	−3.24	5.1	99.95
	4	−1.83	4.9	99.80
	6	−1.22	4.8	99.93
	8	−0.91	4.6	99.81
	10	−0.51	4.3	99.59

To describe the non-isothermal crystallization process of HPBS–SH/PP blends, the Avrami analysis was used [12–14]:

$$\alpha(t) = 1 - \exp(-Kt^n) \quad (1)$$

where $\alpha(t)$ is the relative crystallinity as a function of temperature, K a rate constant involving both nucleation and growth mechanisms, n a parameter, which also depends on the type of nucleation and the geometry of the growth process parameters, and t the crystallization time that can be determined as a function of crystallization temperature T and cooling rate β:

$$t = (T_0 - T)/\beta \quad (2)$$

Plotting $\log[-\ln(1 - \alpha(t))]$ versus $\log(t)$ in Fig. 6, all the lines are parallel to each other, which means that the Avrami equation is satisfied. The values of intercept and slope determined from the linear regression are, respectively, log K and the Avrami exponent n. All the data are listed in Table 3; the obtained correlation coefficients (R) are >99% for all the fits.

The values of *log K* obtained show that the crystallization rate increases with an increase in cooling rate for a given blend composition and decreases with the increase in PP content in the blends for a given cooling rate.

The value of the Avrami exponent n contains information on nucleation and growth geometry. Its interpretation may be complicated due to the mechanisms involved during the process. As can be seen in Fig. 7, the general tendency in

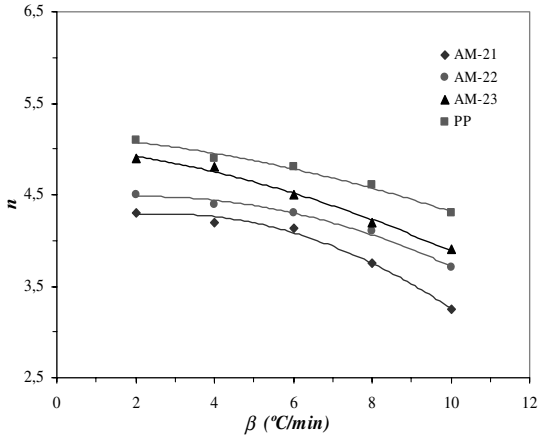

Fig. 7. Plot of Avrami exponent n versus cooling rate β, for non-isothermal crystallization of PP pure and in HPBS–SH/PP blends with different PP content.

this case, is a decrease of n by increasing cooling rate and PP content in the blends. This behavior can be explained by changes in growth geometry when cooling rates are varied.

The tendency for changes in n observed in Fig. 7 are due to the transition between heterogeneous and homogeneous nucleation [15]. When low scanning rates were used, the value of the Avrami exponent was close to 4, which suggested that the non-isothermal crystallization of PP in HPBS–SH/PP blends correspond to a three-dimensional growth with homogeneous nucleation. For higher scanning rates, n was close to 3, which can be attributed to heterogeneous nucleation of a three-dimensional growth.

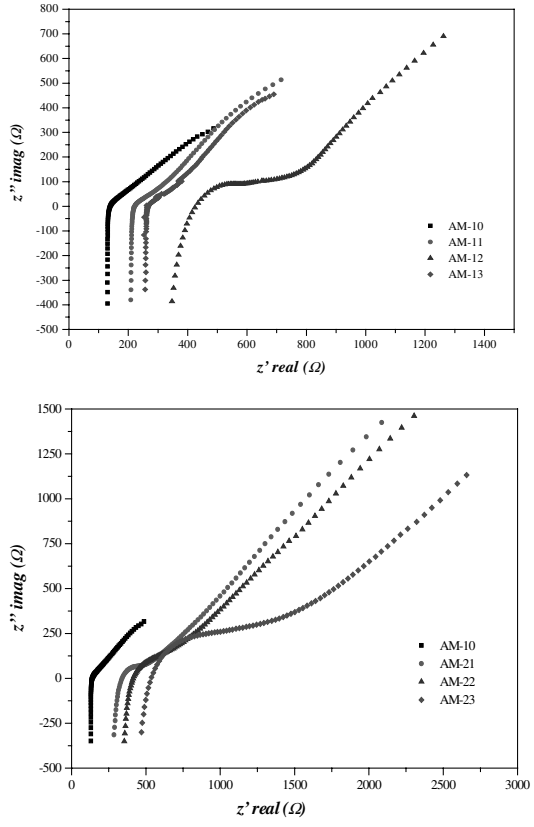

Fig. 8. Impedance spectra obtained for HPBS–SH/HPBS and HPBS–SH/PP blends, after 1hour hydration at 50°C. AC mode. Amplitude of applied signal 1 V. Frequency range 0.01–10 000 kHz.

Table 4
Conductivity data before and after hydration

Sample	Conductivity (Ω^{-1} cm^{-1})	
	Before hydration	1 h hydration at 50°C
AM-10	9.40×10^{-7}	8.10×10^{-3}
AM-11	3.99×10^{-7}	9.92×10^{-3}
AM-12	8.29×10^{-7}	6.15×10^{-3}
AM-13	7.15×10^{-7}	1.12×10^{-3}
AM-21	2.67×10^{-8}	5.07×10^{-3}
AM-22	1.47×10^{-8}	3.06×10^{-3}
AM-23	1.34×10^{-8}	1.63×10^{-3}

3.4. Conductivity analysis

Ion conductivity of proton conducting membrane was determined using the complex impedance method. Impedance spectrum, shown in Fig. 8, comprises two well-defined regions, a high-frequency zone that is related to conduction processes in the bulk of the sample, and a low-frequency region, which is attributed to the solid electrolyte–electrode interface. The bulk resistance is obtained from the intercept of high-frequency curves with the real axis. This resistance is smaller for samples with higher conductivities.

All impedance measurements were done after 1 h hydration at 50°C of the films. Since the blends in dry form exhibit conductivities between 10^{-8} and 10^{-7} Ω^{-1} cm^{-1}, the entire conduction process occurs through water incorporated in the polymer structure. Data obtained before and after hydration are presented in Table 4.

In Fig. 9, isotherms at 50°C of ionic conductivity of HPBS–SH blends as a function of HPBS and PP concentrations are

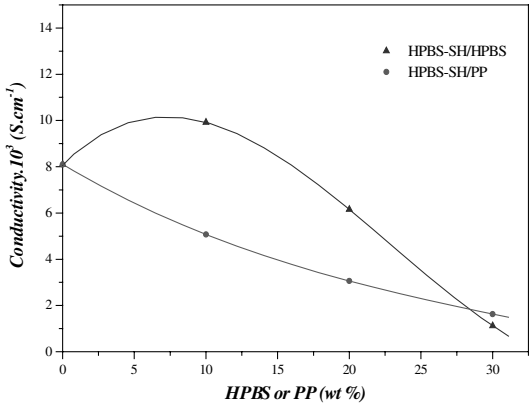

Fig. 9. Isotherms of the ionic conductivity of HPBS–SH blends as a function of HPBS and PP concentration.

plotted. In the case of HPBS–SH/HPBS blends, conductivity increases when 10% HPBS was added, and decreases for higher concentrations. While for HPBS–SH/PP blends, conductivity decreases with increasing PP concentration.

4. Conclusions

Sulfonated hydrogenated polybutadiene styrene polymer HPBS–SH, was prepared by partially sulfonating the styrene blocks. FTIR spectroscopy was used to confirm that styrene sulfate was the reaction product.

DMA analyses show that glass transition temperature of PS domain, increases 30°C after sulfonation, while T_g of hydrogenated polybutadiene phase remains practically constant.

For HPBS–SH/HPBS blends, $T_{g(PS)}$ decreases when the amount of HPBS added increases. In addition, higher proton conductivity was measured when 10 wt.% HPBS was added, and decreases for superior concentrations.

In the case of HPBS–SH/PP blends, some changes in high T_g of HPBS–SH are observed, whose origin is not fully understood. Moreover, diminution in proton conductivity was also observed on increasing the PP content of the films.

The study of kinetics of non-isothermal crystallization of PP in HPBS–SH/PP blends, using Avrami analysis, show that for low scanning rates (<8°C/min), the Avrami exponent was ≥ 4 and coincides with a three-dimensional growth with homogeneous nucleation. For higher scanning rates, n was close to 3 and could be attributed to heterogeneous nucleation.

Acknowledgements

The support of Repsol, European Community and Comunidad Autonoma de Madrid (CAM) is gratefully acknowledged.

References

[1] Jun YK, Seong HK. Solid State Ionics 1999;124:91–9.
[2] Blythe AR. Electrical properties of polymers. New York: Cambridge University Press, 1979.
[3] Gray FM. Solid polymer electrolytes, fundamentals and technological applications. New York: VCH Publishers, 1991.
[4] Harsanyi G. Polymer films in sensor applications. Lancaster-Basel (USA): Technomic Publishing, 1995.
[5] Weiss RA, Sen A, Pottick LA, Willis CL. Polymer 1991;32(15): 2785–92.
[6] Weiss RA, Sen A, Willis CL, Pottick LA. Polymer 1991;32(10): 1867–74.
[7] Nishida M, Eisenberg A. Macromolecules 1996;29:1507–15.
[8] Kim JS, Nishida M, Eisenberg A. Polymer Journal 1999;31(1):96–8.
[9] Eisenberg A, Kim JS. Introduction to ionomers. Wiley, 1998.
[10] Makowski HS, et al. US Patent, 3 (1975) 870,841.
[11] Makowski HS, et al. US Patent, 4 (1980) 184,988.
[12] Avrami M. Journal of Chemistry and Physics 1939;7:1103–9.
[13] Avrami M. Journal of Chemistry and Physics 1940;8:212–21.
[14] Avrami M. Journal of Chemistry and Physics 1941;9:177–85.
[15] Di Lorenzo ML, Silvestre C. Progress in Polymer Science 1999;24: 917–50.